Dynamic Light Scattering Study of Structural Changes of Cellulose Diacetate in Solution under Couette Flow

Hiroyuki Kawanishi, Yoshisuke Tsunashima,* and Fumitaka Horii

Institute for Chemical Research, Kyoto University, Uji, Kyoto 611-0011, Japan

Received August 4, 1999; Revised Manuscript Received January 5, 2000

ABSTRACT: Dynamic light scattering (DLS) measurements were conducted under a simple shear flow, i.e., the Couette flow field, to cellulose diacetate (CDA; a typical polysaccharide) in semidilute *N*,*N*-dimethylacetamide (DMAc) solution. The shear rate γ was varied from 0 to 5.25 s^{-1}. At quiescence, CDA showed three dynamic modes, which correspond to two kinds of associations and a single chain. In the weakly sheared system (0.402 $s^{-1} \leq \gamma \leq 5.25$ s^{-1}), the three dynamic modes collapsed, and alternatively two completely different modes were observed. The fast mode experienced a transition around $\gamma = 0.81$ s^{-1}, the decay rate distribution changing from a broader bimodal to a narrower unimodal shape with increasing shear. The slow mode had a unimodal decay rate distribution, but the length scale of fluctuations was larger by 3 orders of magnitude compared to those observed at $\gamma = 0$ s^{-1}; that is, the length distribution was extremely uniform irrespective of γ, and the length ξ_s was proportional to γ^{-1}. This $\xi_s \propto \gamma^{-1}$ relation was interpreted by Taylor's treatment of the behavior of viscous drops. Thus, the repetition of the burst and the coalescence growth of the associations was suggested for the slow mode. The $\xi_s \propto \gamma^{-1}$ relation implied that CDA was molecularly disperse in DMAc under the viscometric field in a capillary viscometer at $\gamma = 920$ s^{-1}.

I. Introduction

It is well-known[1−3] that cellulose and cellulose derivatives form clusters in solution due to their crystallinity, but detailed studies of this complex solution behavior have not been conducted adequately. Recently, many studies have been reported on the complex aggregation phenomena in cellulose[1,3−5] and cellulose derivative[2,6−10] solutions using different techniques. Cellulose diacetate (CDA) is a cellulose derivative,[11] where about two of the three hydroxyl groups per a glucose residue are substituted by *O*-acetyl groups. The solubility in various solvents depends on the degree of substitution (DS).[11] In aprotic polar solvents, CDA may exhibit intra- or intermolecular hydrophobic and/or hydrophilic interactions through the substituted groups or the glucose residues. In *N*,*N*-dimethylacetamide (DMAc), CDA exhibits the particular solution behavior[12−15] described below.

We have first shown[13] through dynamic light scattering (DLS) measurements that, even in the dilute solution of CDA in DMAc in the quiescent state, temporary clusters are formed due mainly to a long-range interaction such as a hydrogen bond between molecules directly or via solvents. In other words, two relaxations of concentration fluctuations appear in dilute solution and coexist with the translational, or the center-of-mass, diffusion of single CDA molecules. These two concentration fluctuations were found to be created by a nested mechanism of a creation−dissipation process of locally but temporarily clustered CDA molecules in DMAc.[13] These dynamic structures were dependent on polymer concentration[13] and temperature.[15] In semidilute solution a new cooperative mode was observed,[14] which was never seen in usual neutral polymer solutions.[16,17] Moreover, it was found that CDA was molecularly dispersed only under external fields such as the shear viscous and the ultracentrifugal fields.[12] However, the persistence length estimated in DMAc by the Yamakawa−Fujii−Yoshizaki theory[18,19] was 8 nm in the viscometric fields, whereas it was 43 nm in the ultracentrifugal fields. This discrepancy in the persistence length between viscometric and ultracentrifugal fields has not been reported so far for usual stiff polymers in solution,[20,21] but it seems to be most pronounced for CDA.[12] The discrepancy thus shows that a CDA chain is much stiffer in the ultracentrifugal field than in the viscometric field and that the chain stiffening is due to additional intramolecular hydrogen bonding.[12] Molecular dynamic (MD) simulations of cellobiose in the quiescent state, where the solvent effect was included, have recently shown[22] that the chain conformation of dissolved cellulose contains a few percent of abnormal ring conformations, e.g., the boat or inverted chair conformations, and that these conformations cause sensitively a decrease in the persistence length of cellulose. This decrease of the abnormal ring conformations may induce the increase in the persistence length observed for CDA in DMAc. However, since there are only a few percent[22,23] or less[24] of abnormal ring conformations in cellulose (if they exist), it seems difficult to attribute the chain stiffening in CDA to their absence or reduced frequency.

The facts mentioned above expose the dynamic feature of CDA in DMAc; CDA forms two kinds of associations and contains also single chains in the quiescent state, but it is exclusively in the molecular dispersion state in shear viscous fields of $\gamma = 920$ s^{-1}.[12] Therefore, it is very interesting to examine in the intermediate external fields ($0 < \gamma < 920$ s^{-1}) the influence of external shearing forces on cluster formation in the CDA/DMAc system. In this paper, we applied the DLS method under shear flow[25−27] to the semidilute CDA/DMAc solutions. The shear rate imposed on the system was in $0 \leq \gamma \leq 5.25$ s^{-1}, much less than that in the viscometric and ultracentrifugal fields. There are a few DLS studies on

* To whom correspondence should be addressed. E-mail: tunasima@molmat.kuicr.kyoto-u.ac.jp.

10.1021/ma9913055 CCC: $19.00
Published on Web 03/01/2000

the polymer chain dynamics under a simple shear flow,[25−30] but to our best knowledge, the present work is the first to observe complex dynamics in *associating* polymers in solution. We aimed to obtain information about shear effects on dynamics of the polymer/solvent system where the polymer associates by hydrogen bonding. We also addressed the question how strong a shear rate was needed to obtain molecularly dispersed CDA. We compared the behavior of the CDA/DMAc system under shear flow with results of previous studies.

II. Experimental Method

The CDA sample, coded as Fr.1C, was a fractionated sample prepared by successive precipitation fractionation of a commercial CDA product (CDA8, Daicel Chemical Industries, Ltd.) with DMAc as a solvent and methanol as a precipitant. Its weight-averaged molecular weight was $M_w = 1.70 \times 10^5$ g mol^{-1}, the degree of substitution was DS = 2.44, the polydispersity index was $M_z/M_w = 1.23$, and the second virial coefficient and the intrinsic viscosity were $A_2 = 1.21 \times 10^{-3}$ cm^3 mol g^{-2} and $[\eta] = 305$ cm^3 g^{-1}, respectively, at 30 °C.[12,13] The polymer mass concentration c was 5.57×10^{-3} g cm^{-3}, which corresponds to the crossover of dilute and semidilute solution with $c/c^* = 1.70$, where c^* is the overlap concentration calculated from the relation $c^* = 1/[\eta]$. The stock solution prepared was filtered into a scattering cell through a 0.2 μm pore-size filter (Sartorius) and was kept in a thermostat-controlled box with intermittent stirring. The DLS measurements were conducted through multiple tau digital correlator (ALV-5000/E) using vertically polarized incident light of the single-frequency 488 nm line emitted from an etalon-equipped Ar ion laser (3 W, Spectra Physics) at 27 °C. The solutions for DLS under shear were filtered into the 2 mm gap between the inner rotating and the outer stationary glass cylinders. The details of the flow-DLS apparatus have been described elsewhere.[25−27] The vertical component of the scattered light was detected at the scattering angle 75.6°. The intensity−time correlation function $g^{(2)}(t)$ was analyzed by the inverse Laplace transformation (CONTIN[31,32]) program, where the electric field time correlation function $g^{(1)}(t)$ given by the Siegert relation, $g^{(2)}(t) = 1 + |g^{(1)}(t)|^2$, was expressed by the multiple sum of single-exponential decay functions $g^{(1)}(t) = \sum_j a_j \exp(-\Gamma_j t)$ with Γ_j the decay rate and a_j the amplitude for the jth decay function.[32] If the distribution of the decay rate can be deduced to several separated peaks, we designate each as mode i (i = s, f, ...) of the *mean* decay rate Γ_i and of the *mean* relaxation time τ_i (=$1/\Gamma_i$):

$$g^{(1)}(t) = \sum_i A_i \exp(-\Gamma_i t) \qquad (1)$$

Here Γ_i and A_i are averaged only over the separated peak (= mode) i.

III. Results and Discussion

A. Time Correlation Functions in Quiescent State and in Simple Shear Flow. Figure 1 shows the intensity−time correlation functions $g^{(2)}(t)$ observed at $\theta = 75.6°$ in (a) the quiescent state, measured for 60 min, and (b) $\gamma = 0.402$ s^{-1}, the lowest γ, for 10 min. The difference is obvious. In the case of the quiescent solution (Figure 1a), $g^{(2)}(t)$ decays over the time range from 3×10^{-3} to 4 ms with a large amplitude, and as is given by a data-fitted solid line, it deduces a triple sum of single-exponential decays, i.e., three discrete and narrow decay rate distributions (Figure 2a). They were assigned,[13] from right to left, to the self-diffusion motion of a single CDA molecule (mode I) and to two dissipation processes of locally and temporally associated CDA clouds (modes II and III). The latter processes were

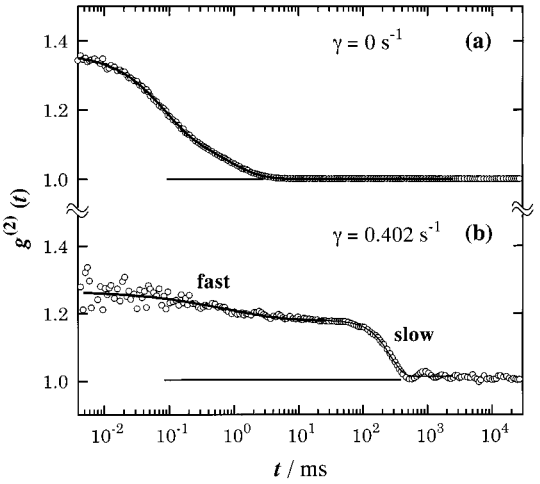

Figure 1. Normalized time correlation function $g^{(2)}(t)$ plotted against logarithmic time t for CDA in DMAc at the shear rate (a) $\gamma = 0$ s^{-1}, the quiescent state, and (b) $\gamma = 0.402$ s^{-1}, the lowest shear rate measured. $c = 5.57 \times 10^{-3}$ g cm^{-3}, $\theta = 75.6°$, and $T = 27$ °C. The solid thick lines represent the best-fit curves expressed by numerous numbers of single-exponential decays (the CONTIN method for (a) $\gamma = 0$ s^{-1} over the full range and (b) $\gamma = 0.402$ s^{-1} over the time range of 5×10^{-3}−20 ms, which corresponds to the fast mode. The solid thin line in (b) represents the result for the slow mode, which was analyzed by the KWW type of the decay function (for details, see the text).

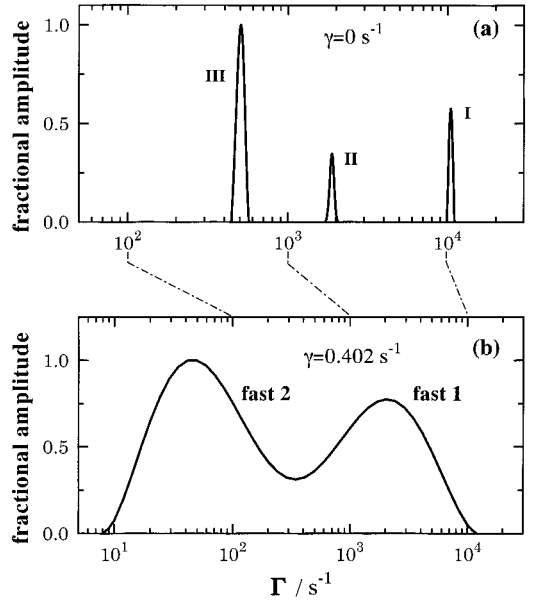

Figure 2. Distributions of the decay rate Γ for the CDA/DMAc solution of $c = 5.57 \times 10^{-3}$ g cm^{-3} at $\theta = 75.6°$ and $T = 27$ °C. (a) The triple sharp distribution in the quiescent state ($\gamma = 0$ s^{-1}, see Figure 1a). (b) The bimodal broad distribution for the fast mode at $\gamma = 0.402$ s^{-1} (see the solid line in Figure 1b). It should be noted that the time ranges depicted in (a) and (b) are different. The chain lines indicate the same Γ ranges corresponding to (a) and (b).

bound by hydrogen bonding between neighboring chains in the aprotic polar solvent.

In the sheared system at $\gamma = 0.402$ s^{-1} (Figure 1b), the decay is extended over a very large time region, and the oscillating structure develops in $g^{(2)}(t)$, which never results from the ambiguity of date sampling as described below. The extremely sharp decay with a large amplitude appears in the time range 70−600 ms, which is larger by 3−4 decades as compared to the result at $\gamma = 0$. We call it the slow mode. We can also see another

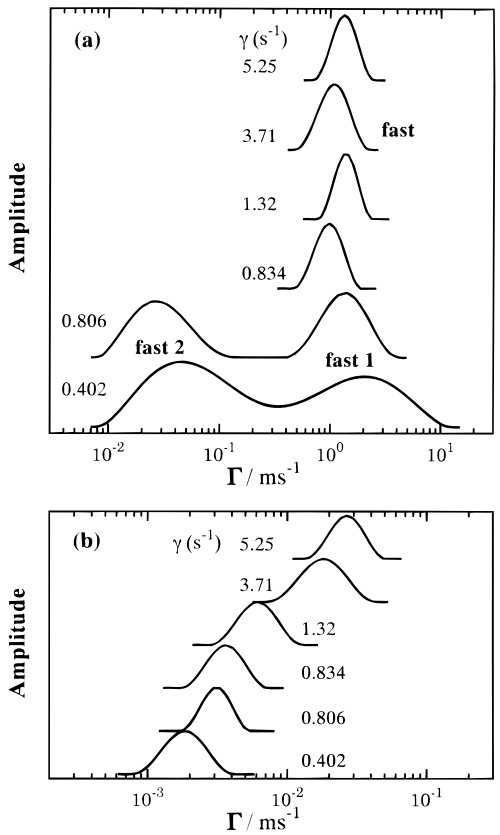

Figure 3. Decay rate distributions for (a) the fast mode and (b) the slow mode at $\gamma = 0.402$, 0.806, 0.834, 1.32, 3.71, and 5.25 s^{-1}, from bottom to top. These are obtained by the CONTIN method.

mild decay (fast mode) with a small amplitude in the short time region of 3×10^{-3}−20 ms. As shown more in detail later, this time range is little shifted from that of the quiescent state, but the decay rate distribution results not in three discrete peaks but in a very broad one, as shown in Figure 2b by a quasi-bimodal peak. Here we note that the short-time data in the fast mode region contain the oscillatory component of large amplitudes. However, it is found that the oscillation damps with a regular cycle if the data are plotted (though not shown here) against time t, not against log t as in Figure 1. Since there are little noises in this oscillating cycle, the analysis of $g^{(2)}(t)$ in the fast mode region can be systematically performed in consideration of this damping oscillation. We thus pursued this analytical process and applied it also to the case of the slow mode region, where another oscillation with a regular cycle is observed. As a result, the slow and fast modes under shear flow resulted into sum of numerous single-exponential decays. The fast mode was well represented by this procedure as seen by the data fitted solid thick line in Figure 1b, but the slow mode was not, because of its sharpness in the decay feature. The detail will be discussed later in the part C. The strong oscillatory behavior observed in $g^{(2)}(t)$ in the fast and slow mode regions, which would probably indicate an appearance of the dissipative structures induced by shear, will also be discussed later. In the following, each mode will be described in detail.

B. Fast Mode. Figure 3a shows the distribution function of the decay rate Γ for the fast mode at various shear rates γ. The γ value increases from bottom to top with 0.402, 0.806, 0.834, 1.32, 3.71, and 5.25 s^{-1}. With the increase of γ, the shape of distribution changes: it is a bimodal form at two lower shear rates, $\gamma = 0.402$ and 0.806 s^{-1}, but a single modal form at γ higher than 0.834 s^{-1}. We discuss first the bimodal distributions observed at $\gamma = 0.402$ and 0.806 s^{-1} and then refer to the single distribution at $\gamma \geq 0.834$ s^{-1}. For further elucidation, we distinguish the faster mode with a larger Γ (fast 1) from the slower mode with a smaller Γ (fast 2). At $\gamma = 0.402$ s^{-1}, the decay rate distribution is quasi-bimodal; i.e., fast 1 and fast 2 are not clearly separated, and both spread over the 3 orders of magnitude of Γ (see also Figure 2b). Comparing the distribution with that at quiescence (Figure 2a), we find that the distribution of fast 1 (Figure 2b) covers nearly the same Γ region at $\gamma = 0$, but it is continuous and broad in contrast to the discrete and narrow one at $\gamma = 0$. In addition, fast 2 is induced in the smaller Γ region with a broad distribution. At $\gamma = 0.806$ s^{-1} (Figure 3a), however, the distribution becomes a bimodal form with two completely separated shapes, fast 1 and fast 2, though both shifting slightly to the smaller Γ region. The amplitude of fast 1 also changes; it becomes larger than that of fast 2. Above $\gamma = 0.834$ s^{-1}, the distribution of the fast mode changes drastically in its shape, and a single distribution of relatively narrow width begins to appear. The distribution shape is nearly the same, and the position is settled near the fast 1 mode.

As a result, we can imagine the following picture for the fast mode. At a weak shear as $\gamma = 0.402$ s^{-1}, three dynamic modes in the quiescent CDA/DMAc system which are characterized by the narrow and discrete distributions (Figure 2a) collapse, and alternatively one mode of motion (fast 1) appears, which is characterized by a broad continuous distribution and is located in almost the same Γ region as in quiescence (Figure 2b). At the same time, another mode of motion (fast 2) appears newly in the Γ region, smaller by 2 orders of magnitude than the fast 1, the new one having also the broad and continuous distribution. Both fast 1 and fast 2 are so widely distributed that they overlap (quasi-bimodal) over three orders in Γ. However, as γ increases to 0.806 s^{-1}, the variety of motions decreases, resulting in two broad distributions which are separated from each other by two orders and spread over about three orders in Γ (Figure 3a). As shear increases further, the variety in the motions decreases extremely and the distribution becomes much narrower. In other words, at a shear rate higher than $\gamma = 0.834$ s^{-1}, the slower mode (fast 2) disappears, and only fast 1 remains without peak shift. These results suggest that the two steps of structural transitions occur in CDA in solution between $\gamma = 0$−0.402 s^{-1} and $\gamma = 0.806$−0.832 s^{-1}.

In Figure 4a, the mean relaxation time of concentration fluctuations τ_f defined for the fast mode as $\tau_f = 1/\Gamma_f$ is plotted against the shear rate γ. Here Γ_f is the mean decay rate averaged over the decay rate distribution given by Figure 3a. The symbols △ and ▽ represent the values for fast 1 and fast 2, respectively. The split values at $\gamma \leq 0.806$ s^{-1} converge to a constant one (fast, ○) above $\gamma = 0.834$ s^{-1}, and the transition occurs about $\gamma = 0.806$−0.834 s^{-1}. Thus, the fast 2 mode observed at $\gamma = 0.402$ and 0.806 s^{-1} disappears above $\gamma = 0.834$ s^{-1}. Up to the present, we detected these modes at only one scattering angle and obtained no evidence of the q^2 dependence of Γ, where $\boldsymbol{q}$ is the scattering vector. It is uncertain that the modes obtained under shear are diffusive. However, it is certain that Γ of each mode

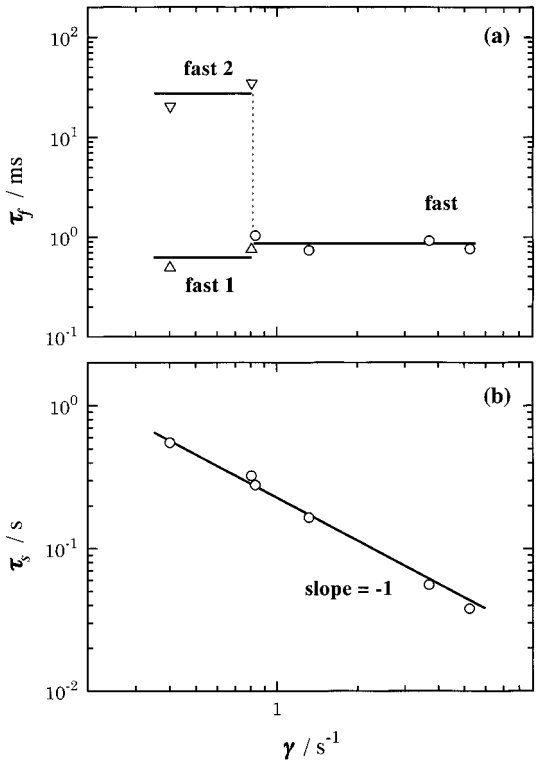

Figure 4. (a) Relaxation time for the fast mode τ_f plotted double-logarithmically against γ. At $\gamma = 0.402$ and 0.806 s^{-1}, fast mode is composed of fast 1 (△) and fast 2 (▽) modes, and at $\gamma \geq 0.834$ s^{-1} they converge to one, fast mode (○). (b) The relaxation time for the slow mode τ_s plotted against γ. τ_s decreases linearly with γ.

reflects the concentration fluctuation of a dynamic structure that is induced temporarily in solution under shear. We thus define, at present, the correlation length of the concentration fluctuation ξ_f as $\xi_f = (q^2 k_B T/6\pi\eta_0)\tau_f$ and obtain $\xi_f = 83 \pm 17$ nm for the fast 1 mode at $\gamma \leq 0.806$ s^{-1} and $\xi_f = 115 \pm 13$ nm for the fast mode at $\gamma \geq 0.834$ s^{-1}. Here η_0 is the solvent viscosity, k_B is the Boltzmann constant, and T is the absolute temperature. Except for fast 2, ξ_f is found to be in the range 83−115 nm, which is comparable to the correlation length of mode II in the quiescent state. This suggests that the fluctuations of dynamic structures in solution are constrained under the simple shear flow so that a suitable structure (fast 1) can remain solely.

Finally, we refer in brief to the oscillatory behavior of $g^2(t)$ at the short-time region. The oscillation period was found to be *constant* irrespective of γ, though the transition occurs in τ_f (Figure 4a). Connecting this constant time rhythm with the τ_f transition, we could imagine that there is a dissipative structure, or a limit cycle, by shear in solution. The migration of temporary aggregations of CDA is inconsistent with the constancy of τ_f.[33] The attractive hydrogen-bond interaction plays an essential role in this oscillatory behavior.

C. Slow Mode. For convenience of imagining the slow mode, we try to fit the sharply decaying slow mode (Figure 1b) by the CONTIN method. A more precise but complicated method of data fitting will be indicated below briefly, but the essence of the dynamics in this mode can be extracted by the CONTIN method. The shear rate dependence of the decay-rate distribution extracted by this method is shown in Figure 3b. At each γ the distribution is of single modal form, the width being almost the same and the peaks shifting to the

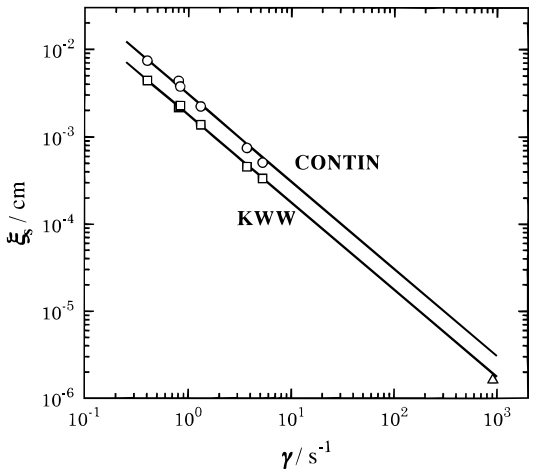

Figure 5. Correlation length of concentration fluctuations for the slow mode, ξ_s, plotted against γ. Analyses were made by the CONTIN (○) and the KWW (□) methods. Both methods give the relation that $\xi_s \propto \gamma^{-1}$, consistent with each other. The hydrodynamic radius R_H of a single CDA chain in infinite dilution is given by an unfilled triangle (△).

smaller decay time τ ($=\Gamma^{-1}$) with the increase of γ. The mean decay time τ_s estimated from the distribution is plotted against γ in the double-logarithmic form in Figure 4b. τ_s decreases linearly with increasing γ with the relation that $\tau_s \propto \gamma^{-1}$. In the crossover concentration region as in the present case, it will be suitable to express τ_s in terms of the correlation length representing the concentration blob or the range over which the concentration fluctuation develops, and we define it by $\xi_s = (q^2 k_B T/6\pi\eta_0)\tau_s$. The relation $\tau_s \propto \gamma^{-1}$ then gives $\xi_s \propto \gamma^{-1}$. As shown in Figure 5, ξ_s gives a very large value, and it changes from 74 to 5.1 μm with a decrease in γ from 0.402 to 5.25 s^{-1}. In what follows, we will propose a mechanism that induces this behavior and examine the properties of this very large structure under shear.

According to the mechanism of the elongation and the burst of a single drop of fluid in another kind of fluid under flow, the following relation was proposed by Taylor:[34,35]

$$R^* = C\frac{\sigma}{\eta}\gamma^{-1} \qquad (2)$$

Here R^* is the critical size of a single droplet, σ is the surface tension, η is the shear viscosity, and C is a constant. R^* is determined by a balance between the shear stress tending to burst the droplet and the surface tension tending to induce the droplet to grow. The larger droplet suffers larger hydrodynamic forces from the shear flow, resulting in the burst of the droplet, while the smaller droplet becomes less stable because of the large surface tension, which increases the droplet size. From this viewpoint, the relation given by $\xi_s \propto \gamma^{-1}$ would be realized under a balance of the following three factors: the hydrodynamic forces exerted by flow, the thermodynamic forces relating the interfacial energy, and the association energy of CDA aggregate. Recently, the relation of $\xi_s \propto \gamma^{-1}$ has been predicted[36] theoretically for a critical mixture of two immiscible Newtonian fluids with the same viscosity and observed experimentally for immiscible binary polymer mixtures[37,38] and for phase-separated structures in a semidilute solution of off-critical mixtures.[39] However, it should be noted that these systems mentioned above are different from the

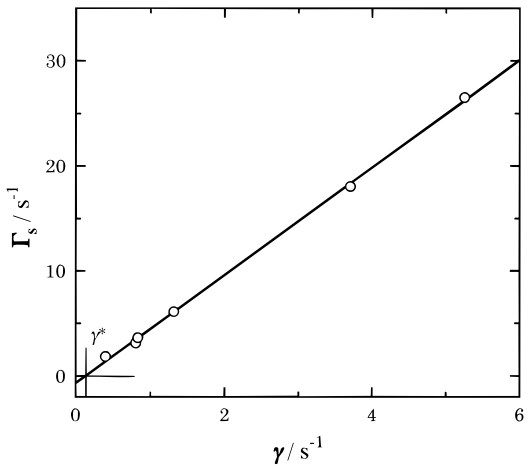

Figure 6. Averaged decay rate for the slow mode Γ_s plotted against γ. The line was obtained by the least-mean-squares fitting. γ^* is a critical γ, above which the slow mode begins to appear.

present CDA/DMAc system in that there is no specific attractive or repulsive interaction in solution.

To represent more precisely the decay feature of the slow mode, we tried to fit the sharply decaying $g^{(2)}(t)$ curve (Figure 1b) by the Kohlrausch−William−Watts (KWW) type of the stretched exponential decay function[40]

$$g^{(2)}(t) = 1 + |g^{(1)}(t)|^2, \quad g^{(1)}(t) = A \exp[-(\Gamma t)^{\beta}] \quad (3)$$

Here β ($0 < \beta \leq 2$) is recognized to be a measure of the sharpness of the decay distribution. In other words, $g^{(1)}(t)$ in eq 3 is a special or a symmetric stable distribution form of the probability measure[41,42] which is derived from the Levi theory in stable distributions in stochastic processes: $\beta \cong 0$ for the very broad log-normal distribution, $\beta = 1$ for the Lorenz or Cauchy one, giving a single-exponential decay form, and $\beta = 2$ for the normal or Gaussian one. The broader the distribution is, the smaller the β value becomes. The Gaussian distribution is thus sharpest in Levi's framework. The result analyzed by the KWW function is demonstrated by the solid thin line in Figure 1b for the solution at $\gamma = 0.402$ s^{-1}. The results for solutions at other γ showed that β was about 2.17 ± 0.15, independent of γ. This means that the decay time distribution for the slow mode takes the sharpest distribution of $\beta = 2$[41,42] and that the distribution form is not affected by shear in the range $0.402 \leq \gamma \leq 5.25$ s^{-1}. The repetition of the burst and the coalescence growth of associations under the shear flow seems to make the fluctuation distribution so narrow as presented by the stretched exponent $\beta = 2$. An extremely uniform distribution, similar to the present one, has been detected under shear for a semidilute solution of off-critical mixtures through *static* light scattering measurements.[39] We should, however, stress again that in our case the sharp distribution may be achieved by a long-range interaction such as a hydrogen bond via solvents. In the Couette flow, it is thus found that the dynamic behavior in the associating CDA/DMAc solution is influenced strongly by a weak shear such as 0.402 s$^{-1} \leq \gamma \leq 5.25$ s^{-1}. Further insight into this feature will be obtained from Figure 6, where Γ_s is plotted against γ in linear scales. Γ_s increases linearly with γ, yielding the relation $\Gamma_s = -0.672 + 5.13\gamma$ (s^{-1}). Since Γ_s should be positive, we obtain $\gamma^* = 0.13$ s^{-1} at $\Gamma_s = 0$. γ^* is a critical shear rate for formation of very large structures and above which the onset of the transition appears in the CDA/DMAc solution. Thus, in quiescent solutions there exist single chains and two kinds of temporary associations with a size of 71 and 270 nm (Figure 2a), but above γ^*, e.g. $\gamma = 0.402$ s^{-1}, a very large structure of 74 μm is formed, larger by 3 orders of magnitude compared to that of associations at $\gamma = 0$. Thus, in the range of $\gamma^* < \gamma < 0.402$ s^{-1}, the effect of shear flow seems to facilitate the development of associations in solution. Very recently, nonequilibrium molecular dynamic simulations under external shear forces have studied the solution behavior of associating telechelic polymers and demonstrated the critical role of the shear in the onset of association.[43]

In connection with the discussion mentioned above, we refer to the oscillatory behavior in the slow mode, which might propose another aspect for understanding the present results. The oscillation period of the slow mode was found to decrease with γ^{-1} and was consistent with the characteristic time scale that is expected essentially from DLS in the Couette flow.[25,33] It is the time scale with which the fluctuation traverses across the scattering volume. This time evolution of concentration fluctuations will be driven by propagation of the attractive hydrogen-bond interaction from one CDA to another via other intermediate CDA molecules. This situation might recall us the spinodal decomposition induced by shear, though it has exclusively been discussed on the time development of the static scattering light intensity after an onset of temperature difference in the measuring system.

Finally, we discuss ξ_s deduced from the CONTIN and the KWW methods. In Figure 5 the ξ_s values deduced from these methods are plotted double-logarithmically against γ. As mentioned already that the two methods are qualitatively consistent with each other, they give the inverse relation between ξ_s and γ :

$$\xi_s = 3.06 \times 10^{-3}\gamma^{-1} \text{ (cm)} \quad \text{(CONTIN)}$$

$$\xi_s = 1.78 \times 10^{-3}\gamma^{-1} \text{ (cm)} \quad \text{(KWW)} \qquad (4)$$

If these relations hold up to a very high shear region, the correlation length of shear-induced structure can be estimated to be $\xi_{s,app} \cong 19$ nm at $\gamma = 920$ s^{-1}; at this shear rate the previous viscosity measurements were conducted in a capillary viscometer.[12] The $\xi_{s,app}$ is compatible satisfactorily to the hydrodynamic radius of a single CDA chain at quiescence, $R_{H,I} = 16.3$ nm, when neglecting the difference between $\xi_{s,app}$ (the value at finite dilution) and $R_{H,I}$ (the value at infinite dilution). This result suggests that, for CDA in DMAc, single chains can be attained only in a shear field as strong as $\gamma = 920$ s^{-1}. This is exactly consistent with previous results deduced from viscosity and ultracentrifugal measurements.[12]

IV. Conclusions

Dynamic light scattering has been conducted to reveal the dynamics of CDA in semidilute DMAc solution in the weak external field or the Couette flow field of $0.40 < \gamma < 5.3$ s^{-1}. It is found that the two temporary associations observed in quiescent state are easily collapsed, and two dynamic structures of different nature are reconstructed. One, called fast mode, has an extremely broad distribution in the length scale of

concentration fluctuations. The distribution changes from a quasi-bimodal to a discrete bimodal and finally, around $\gamma = 0.83\ s^{-1}$, to a sharp unimodal form. Another mode is the slow one, which is newly constructed above the critical γ^* and has a very large length scale. Its distribution, however, is very narrow as is expressed by the exponent $\beta = 2$ of the KWW type of stretched exponential expression. The repetition of the burst and the coalescence growth of associations may induce this slow mode. The length scale of the slow mode, which is expressed by the correlation length, is larger by about 3 orders of magnitude compared to that of associations observed in quiescence. The length is proportional to γ^{-1}, and the relation can be explained by Taylor's treatment of the behavior of viscous drops. At $\gamma \approx 10^3\ s^{-1}$, this relation produces a size compatible to a single CDA chain. This result supports the molecular dispersion of CDA in a viscous shear field of $\gamma \approx 10^3\ s^{-1}$.

References and Notes

(1) Burchard, W. *Trends Polym. Sci. (TRIP)* **1993**, *1*, 192.
(2) Nydén, M.; Söderman, O. *Macromolecules* **1998**, *31*, 4990.
(3) Morgenstern, B.; Kammer, H. W. *Polymer* **1999**, *40*, 1299.
(4) Terbojevich, M.; Cosani, A.; Conio, G.; Ciferri, A.; Bianchi, E. *Macromolecules* **1985**, *18*, 640.
(5) Röder, T.; Morgenstern, B. *Polymer* **1999**, *40*, 4143.
(6) Tanner, D. W.; Berry, G. C. *J. Polym. Sci., Polym. Phys. Ed.* **1974**, *12*, 941.
(7) Klohr, E.; Zugenmaier, P. *Cellulose* **1994**, *1*, 259.
(8) Ilyina, E.; Daragan, V. *Macromolecules* **1994**, *27*, 3759.
(9) Goldszal, A.; Costeux, S.; Djabourov, M. *Colloids Surf. A* **1996**, *112*, 141.
(10) Ostrovskii, D.; Kjøniksen, A. L.; Nyström, B.; Torell, L. M. *Macromolecules* **1999**, *32*, 1534.
(11) Kamide, K.; Saito, M. *Adv. Polym. Sci.* **1987**, *83*, 1.
(12) Kawanishi, H.; Tsunashima, Y.; Okada, S.; Horii, F. *J. Chem. Phys.* **1998**, *108*, 6014.
(13) Kawanishi, H.; Tsunashima, Y.; Horii, F. *J. Chem. Phys.* **1998**, *109*, 11027.
(14) Tsunashima, Y.; Kawanishi, H.; Nomura, R.; Horii, F. *Macromolecules* **1999**, *32*, 5330.
(15) Kawanishi, H.; Tsunashima, Y.; Horii, F. *Polym. Prepr. Jpn.* **1998**, *47*, 3679. In preparation for publication.
(16) de Gennes, P. G. *Scaling Concepts in Polymer Physics*; Cornell University: Ithaca, NY, 1979.
(17) Doi, M.; Edwards, S. F. *The Theory of Polymer Dynamics*; Clarendon: Oxford, 1986.
(18) (a) Yamakawa, H.; Fujii, M. *Macromolecules* **1973**, *6*, 407. (b) *Macromolecules* **1974**, *7*, 128.
(19) Yamakawa, H.; Yoshizaki, T. *Macromolecules* **1980**, *13*, 633.
(20) Norisuye, T. *Prog. Polym. Sci.* **1993**, *18*, 543.
(21) Sato, T.; Teramoto, A. *Adv. Polym. Sci.* **1996**, *126*, 85.
(22) Kroon-Batenburg, L. M. J.; Kruiskamp, P. H.; Vligenthart, J. F. G.; Kroon, J. *J. Phys. Chem. B* **1997**, *101*, 8454.
(23) Hardy, B. J.; Gutierrez, A.; Lesiak, K.; Seidl, E.; Wildmalm, G. *J. Phys. Chem.* **1996**, *100*, 9187.
(24) Marszalek, P. E.; Oberhauser, A. F.; Pang, Y.-P.; Fernandez, J. M. *Nature* **1998**, *396*, 661.
(25) Tsunashima, Y. *J. Phys. Soc. Jpn.* **1992**, *61*, 2763.
(26) Tsunashima, Y. *J. Chem. Phys.* **1995**, *102*, 4673.
(27) Tsunashima, Y. *J. Chem. Phys.* **1999**, *110*, 12211.
(28) Fuller, G. G.; Rallison, J. M.; Schmidt, R. L.; Leal, L. G. *J. Fluid Mech.* **1980**, *100*, 555.
(29) Rusu, D.; Genoe, D.; van Puyvelde, P.; Disdier, E. P.; Navard, P.; Fuller, G. G. *Polymer* **1999**, *40*, 1353.
(30) Hoppenbrouwers, M.; van de Water, W. *Phys. Fluids* **1998**, *10*, 2128.
(31) Proventure, S. W. *Comput. Phys. Commun.* **1982**, *27*, 213; *Comput. Phys. Commun.* **1982**, *27*, 229.
(32) Brown, W.; Nicolai, T. In *Dynamic Light Scattering, The Method and Some Applications*; Brown, W.; Ed.; Clarendon: Oxford, 1993.
(33) Tsunashima, Y.; Kawanishi, H. *J. Chem. Phys.* **1999**, *111*, 3294.
(34) Taylor, G. I. *Proc. R. Soc. London A* **1932**, *138*, 41.
(35) Taylor, G. I. *Proc. R. Soc. London A* **1934**, *146*, 501.
(36) Doi, M.; Ohta, T. *J. Chem. Phys.* **1991**, *95*, 1242.
(37) Takahashi, Y.; Kurashima, N.; Noda, I.; Doi, M. *J. Rheol.* **1994**, *38*, 699.
(38) Takahashi, Y.; Kitada, S.; Kurashima, N.; Noda, I. *Polym. J.* **1994**, *26*, 1206.
(39) Hashimoto, T.; Matsuzaka, K.; Fujioka, K. *J. Chem. Phys.* **1998**, *108*, 6963.
(40) (a) Kohlrausch, R. *Ann. Phys. (Leipzig)* **1854**, *91*, 179. (b) Williams, G.; Watts, D. C. *Trans. Faraday Soc.* **1970**, *66*, 80.
(41) (a) Itoh, K. *Theory of Probability (*in Japanese*)*; Iwanami: Tokyo, 1953. (b) Takayasu, H. *Fractal (*in Japanese*)*; Asakura: Tokyo, 1986.
(42) Takayasu, H. *Prog. Theor. Phys.* **1984**, *72*, 471.
(43) Khalatur, P. G.; Khokhlov, A. R.; Mologin, D. A. *J. Chem. Phys.* **1998**, *109*, 9602.

MA9913055